Available online at www.sciencedirect.com

ScienceDirect

IFAC-PapersOnLine 48-11 (2015) 976–981

On the Performance of a Digital Chaos-Based Communication System in Noisy Channels ⋆

Greta A. Abib * **Marcio Eisencraft** *

* *Polytechnic School of the University of São Paulo, Brazil*
{gaabib,marcio}@lcs.poli.usp.br

Abstract: In recent decades, many papers describing communication systems based on chaotic signals have been published. However, their performance under non ideal conditions needs further investigation. This work evaluates the performance in terms of Bit Error Rate (BER) of a binary communication system, based on chaotic synchronization, when white gaussian noise is added to the transmitted signal. Furthermore, we propose an encoding function that allows controlling the trade-off between how apparent is the message in the transmitted chaotic signal and BER performance.

Keywords: Chaotic Dynamics and Applications; Digital Communications; Synchronization; Dynamical Systems; Bit Error Rate.

1. INTRODUCTION

A chaotic signal is deterministic, aperiodic, bounded in amplitude and it has sensitive dependence on initial conditions (Alligood et al., 1997). Due to these properties, a large number of research areas are developing applications using chaotic signals, including Telecommunications Engineering (Lau and Tse, 2003; Eisencraft et al., 2012). With the frequent emergence of new challenges and applications in this area, studying new techniques and ideas that do not fit in current commercial standards is relevant as a research object. Examples of applications of chaotic signals in the Telecommunications field that have recently come up are: pseudorandom sequences generation (Rovatti et al., 2004), digital communications (Eisencraft et al., 2012, 2013; Ren et al., 2013), ultrawideband communications (Dmitriev et al., 2006), optical communications (Argyris et al., 2005), satellite networks (Grzybowski et al., 2010), device modeling (Soriano et al., 2012b; Monteiro et al., 2009), among many others (Kennedy et al., 2000; Grzybowski et al., 2011).

By one hand, these signals show up suitable for use in applications that require security due to their difficulty of prediction and to the fact that they can be easily confused with the channel noise (Lau and Tse, 2003). Chaotic signals have been proposed as broadband carriers transmitting information with the potential of providing a high level of robustness and privacy in data transmission. For example, Argyris et al. (2005) describe a practical optical high speed communication system using synchronization of chaotic signals in a commercial fiber optic channel where dispersion effects were compensated in a non-adaptive manner.

By the other hand, chaos-based systems that rely on chaotic synchronization present, in general, poor performance in terms of Bit Error Rate (BER) when the channel conditions are not almost ideal (Williams, 2001). For instance, the system as proposed by (Argyris et al., 2005) would perform badly in a wireless channel where distortions vary constantly in time due to multipath, changing noise sources, and other time-variant impairments. In addition, there must be compatibility between chaos-based and conventional communication systems (Lau and Tse, 2003). Thus, there seems to be much research to be conducted before chaotic signals have actual conditions of practical utilization (Eisencraft et al., 2012).

In this article, we numerically analyze the chaos-based communication system proposed by Wu and Chua (1993), in its discrete-time version (Eisencraft et al., 2009). In this system, the message is mixed with a state variable of the transmitter system, through an invertible encoding function. The result is then transmitted and also fed back in the transmitter. This system can be considered as a simplified model of one of the practical implementations of Argyris et al. (2005). The communication channel is modeled as additive white gaussian noise (AWGN).

Furthermore, we propose a different encoding function that permits to control the mix between chaotic and information signals, thus providing a compromise between message security and BER performance.

This article is organized as follows: in Section 2, the digital communication system studied is briefly described. In Section 3, we present the employed maps. Next, in Section 4, the obtained simulation results are shown and finally, in Section 5, we draft some conclusions.

⋆ This work was partly supported by FAPESP under Grant 2014/04864-2 and by CNPq under Grants 311575/2013-7 and 479901/2013-9.

10.1016/j.ifacol.2015.09.319

2. THE DISCRETE-TIME WU AND CHUA COMMUNICATION SYSTEM

The communication system under study is based on the master-slave synchronization method of Wu and Chua (1993) adapted for discrete-time by Eisencraft et al. (2009).

Consider a master system that can be expressed as

$$\mathbf{x}(n+1) = \mathbf{A}\mathbf{x}(n) + \mathbf{b} + \mathbf{f}(\mathbf{x}(n)), \tag{1}$$

and a slave one, which depends on $\mathbf{x}(n)$, and can be written as

$$\mathbf{y}(n+1) = \mathbf{A}\mathbf{y}(n) + \mathbf{b} + \mathbf{f}(\mathbf{x}(n)), \tag{2}$$

where $n = 0, 1, 2, 3 \ldots$, $\{x(n), y(n)\} \subset \mathbb{R}^K$, $\mathbf{x}(n) = [x_1(n), \ldots, x_k(n)]^T$ and $\mathbf{y}(n) = [y_1(n), \ldots, y_k(n)]^T$. Matrix $\mathbf{A}_{K\times K}$ and vector $\mathbf{b}_{K\times 1}$ are constants. The function $\mathbf{f}(\cdot) : \mathbb{R}^K \to \mathbb{R}^K$ is non-linear in general.

Master and slave systems are *completely synchronized* (Boccaletti et al., 2002) when the synchronization error, $\mathbf{e}(n) \triangleq \mathbf{y}(n) - \mathbf{x}(n)$ tends to zero with n, i.e., $\lim_{n\to\infty} \mathbf{e}(n) = \mathbf{0}$. Using (1)-(2),

$$\mathbf{e}(n+1) = \mathbf{y}(n+1) - \mathbf{x}(n+1) = \mathbf{A}(\mathbf{y}(n) - \mathbf{x}(n)) = \mathbf{A}\mathbf{e}(n). \tag{3}$$

So, for the synchronism, it is sufficient that the eigenvalues λ_i of $\mathbf{A}$ satisfy (Agarwal, 1992)

$$|\lambda_i| < 1,\ 1 \le i \le K. \tag{4}$$

A communication system based on (1)-(2) was proposed by Eisencraft et al. (2009), assuming that $\mathbf{f}(\mathbf{x}(n)) = [f(x_1(n)), 0, \ldots, 0]^T$. In this system, the message to be transmitted $m(n)$ is encoded by the signal $x_1(n)$ using an invertible encoding function $c(\cdot,\cdot)$. Thus, the transmitted signal is $s(n) = c(x_1(n), m(n))$. This signal is fed back into the master instead of $x_1(n)$.

The block diagram of this communication system is depicted in Figure 1, where z^{-1} denotes the delay operator (Oppenheim and Schafer, 2009).

The equations governing this system as a whole take the same form of (1) and (2), the only difference being the arguments of $\mathbf{f}(\cdot)$:

$$\mathbf{x}(n+1) = \mathbf{A}\mathbf{x}(n) + \mathbf{b} + \mathbf{f}(s(n)), \tag{5}$$

$$\mathbf{y}(n+1) = \mathbf{A}\mathbf{y}(n) + \mathbf{b} + \mathbf{f}(r(n)), \tag{6}$$

where $r(n)$ represents the signal delivered to the receiver input, that is $r(n) = s(n) + w(n)$, where $w(n)$ is the noise added in the channel, modeled as AWGN.

The retrieved message $m'(n)$ is decoded in the receiver as

$$m'(n) = d(y_1(n), r(n)), \tag{7}$$

with $d(\cdot,\cdot)$ the inverse of $c(\cdot,\cdot)$ with respect to the second variable.

For an ideal channel, i.e., without the presence of noise, $s(n) = r(n)$ and we can write (5) and (6) as

$$\mathbf{x}(n+1) = \mathbf{A}\mathbf{x}(n) + \mathbf{b} + \mathbf{f}(s(n)), \tag{8}$$

$$\mathbf{y}(n+1) = \mathbf{A}\mathbf{y}(n) + \mathbf{b} + \mathbf{f}(s(n)). \tag{9}$$

In this case, the error dynamics is again given by (3), and if condition (4) is satisfied, $\mathbf{y}(n) \to \mathbf{x}(n)$, and in particular, $y_1(n) \to x_1(n)$. Thus, it follows that

$$m'(n) = d(y_1(n), s(n)) \to d(x_1(n), s(n)) = m(n). \tag{10}$$

Therefore, when the communication channel is ideal, message $m(n)$ can be perfectly recovered at the receiver. However, when noise is added to the channel, $s(n) \ne r(n)$ and the recovered message can contain errors.

We consider the encoding and decoding pair c, d calculated for each n as

$$\begin{cases} s = c(x_1, m) = (1-\gamma)\cdot x_1 + \gamma \cdot m \\ m' = d(y_1, r) = (r - (1-\gamma)\cdot y_1)/\gamma \end{cases}, \tag{11}$$

where $0 < \gamma \le 1$ is a constant. This function is a more general version of the mix usually considered in previous work that considered γ fixed and small, see (Eisencraft et al., 2009; Cuomo and Oppenheim, 1993; Cuomo et al., 1993). The parameter γ controls the relative strength of message and chaos in the transmitted signal.

We consider digital messages $m(n) = \pm 1$ for each n. It can be interpreted as the discrete-time low-pass equivalent of a polar modulation (Lathi and Ding, 2009). The symbols are equiprobable. This way, it was added a comparator at the receiver in Figure 1, to obtain a binary estimate $\hat{m}(n)$ of the transmitted message. For each n, if $m'(n) > 0$, the decision is $\hat{m}(n) = +1$ whereas if $m'(n) < 0$, the decision is $\hat{m}(n) = -1$.

For sake of comparison with conventional systems, it is considered the direct transmission of the signal $m(n)$ through the channel, i.e. $s(n) = m(n)$. This case is called here *without chaos*. Defining the signal-to-noise ratio (SNR) as the average energy per bit divided by the power spectral density of the AWGN, it can be shown that, the BER for this case ($\mathrm{BER_{wc}}$ or BER *without chaos*) is given by (Lathi and Ding, 2009)

$$\mathrm{BER_{wc}} = Q\left(\sqrt{\mathrm{SNR}}\right) \tag{12}$$

where

$$Q(y) = \frac{1}{\sqrt{2\pi}} \int_y^\infty e^{-x^2/2} dx. \tag{13}$$

3. CONSIDERED MAPS

In this section we present the maps employed in the simulations. We chose well-known maps of different dimensions in order to test the influence of this choice in terms of BER performance.

The chosen maps must meet the following prerequisites:

(1) they should generate chaotic signals. The maps chosen satisfy this condition (see e.g. (Alligood et al., 1997));
(2) it should be possible to rewrite them as (1);
(3) they must attain master-slave synchronization. For this, the eigenvalues of the associated $\mathbf{A}$ must satisfy (4).

3.1 Quadratic map

The one-dimensional quadratic map, which consists of the logistic map with a change of coordinates (Alligood et al., 1997), is given by

$$x_1(n+1) = -2x_1^2(n) + 1, \tag{14}$$

with $x_1(0) \in [-1, 1]$. This map can be rewritten in the form of (1) with $K = 1$, $\mathbf{A} = 0$, $\mathbf{b} = 1$ and $\mathbf{f}(\mathbf{x}(n)) = \left[-2x_1^2(n)\right]$.

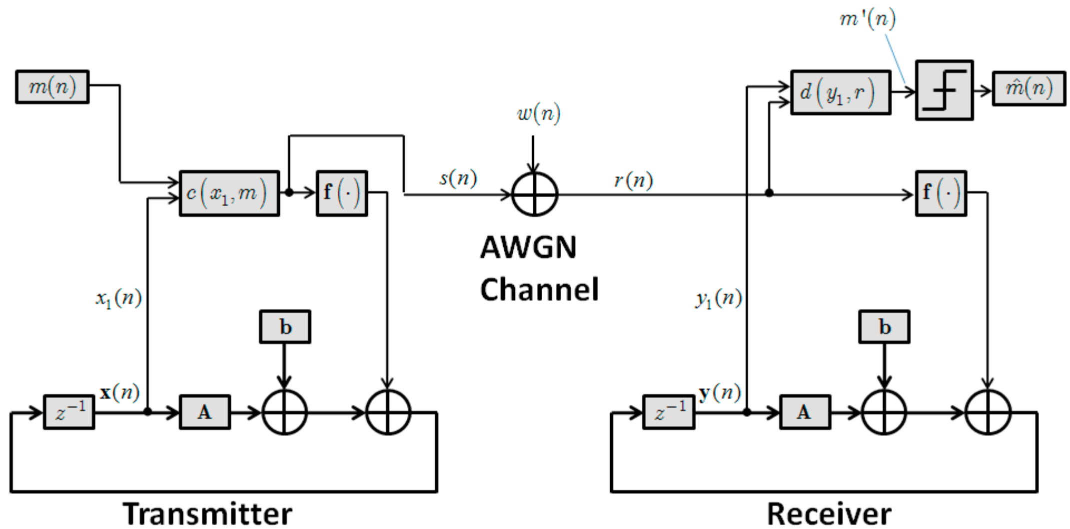

Fig. 1. Communication system under consideration: block diagram.

Thus, for this system, the eigenvalue of $\mathbf{A}$ is $\lambda_1 = 0$ and therefore it satisfies (4). Hence, a master-slave system formed using this map, reaches synchronization.

3.2 Skew tent map

The skew tent map is composed of two linear sections with different slopes signals (Eisencraft et al., 2010). The x-coordinate α of the tent peak is the parameter that defines a map in the family. Thus, maps of the skew tent family are defined by

$$x_1(n+1) = f_I(x_1(n)) = \begin{cases} \dfrac{2}{\alpha+1}x_1(n) + \dfrac{1-\alpha}{\alpha+1}, & -1 < x < \alpha, \\ \dfrac{2}{\alpha-1}x_1(n) - \dfrac{\alpha+1}{\alpha-1}, & \alpha \le x < 1 \end{cases} \tag{15}$$

with $\{\alpha, x(0)\} \subset U = (-1, 1)$. They can be rewritten as (1) with $K = 1$, $\mathbf{A} = 0$, $\mathbf{b} = 0$ e $\mathbf{f}(\mathbf{x}(n)) = [f_I(x_1(n))]$. So, again $\lambda_1 = 0$ and the condition (4) is satisfied. Therefore, a master-slave system formed using this map reaches complete synchronization. For the numerical simulations we considered $\alpha = 0.1$.

It should be noticed that, in fact, any one-dimensional map can be used in the proposed scheme with $K = 1$, $\mathbf{A} = 0$ and $\lambda_1 = 0$. For these maps, the synchronization is trivial since the only state variable is transmitted and therefore directly recovered at the slave.

3.3 Hénon map

The Hénon map (Hénon 2D) is given by (Hénon, 1976)

$$\mathbf{x}(n+1) = \begin{bmatrix} x_1(n+1) \\ x_2(n+1) \end{bmatrix} = \begin{bmatrix} 1 - \alpha x_1^2(n) + x_2(n) \\ \beta x_1(n) \end{bmatrix} \tag{16}$$

and can be rewritten in the form (1) with $K = 2$, $\mathbf{A} = \begin{bmatrix} 0 & 1 \\ \beta & 0 \end{bmatrix}$, $\mathbf{b} = \begin{bmatrix} 1, & 0 \end{bmatrix}^T$, e $\mathbf{f}(\mathbf{x}(n)) = \begin{bmatrix} -\alpha x_1^2(n) & 0 \end{bmatrix}^T$. The eigenvalues of $\mathbf{A}$ are $\lambda_{1,2} = \pm\sqrt{\beta}$, so there is master-slave synchronization for $|\beta| < 1$. For the numerical simulations, we consider $\alpha = 1.4$ and $\beta = 0.3$, as usual in the literature (see e.g. (Alligood et al., 1997)).

3.4 Three-dimensional Hénon Map

A three-dimensional extension of the Hénon map (Hénon 3D) was employed in the study of synchronization of coupled networks of maps (Eisencraft and Batista, 2011). It is given by:

$$\mathbf{x}(n+1) = \begin{bmatrix} x_1(n+1) \\ x_2(n+1) \\ x_3(n+1) \end{bmatrix} = \begin{bmatrix} -\alpha x_1^2(n) + x_3(n) + 1 \\ -\beta x_1(n) \\ \beta x_1(n) + x_2(n) \end{bmatrix}, \tag{17}$$

with $\alpha = 1.07$ and $\beta = 0.3$. It can be rewritten as (1) with $K = 3$, $\mathbf{A} = \begin{bmatrix} 0 & 0 & 1 \\ -\beta & 0 & 0 \\ \beta & 1 & 0 \end{bmatrix}$, $\mathbf{b} = \begin{bmatrix} 1, & 0, & 0 \end{bmatrix}^T$ and $\mathbf{f}(x(n)) = \begin{bmatrix} -\alpha x_1^2(n), & 0, & 0 \end{bmatrix}^T$. The eigenvalues of $\mathbf{A}$ are $\lambda_{1,2} = 0.4084 \pm 0.4477j$, and $\lambda_3 = -0.8169$. As $|\lambda_i| < 1, i = 1, 2, 3$, (4) is satisfied.

Figure 2, shows samples of transmitted signals $s(n)$ for the considered maps. In each case, $m(n)$ is formed by the same equiprobable sequence of ± 1 shown in Figure 2(a).

4. NUMERICAL SIMULATIONS

Using the communication system with the maps and encoding function described in the previous sections, we performed the simulations presented next.

On one hand, to exemplify the influence of the parameter γ in the “security” of the transmitted signal, we show in Figure 3 a message encoded using the quadratic map, the same initial conditions and the encoding function (11) with different values of γ. It can be seen that for values of γ closer to the unity the encoded signal is similar to $m(n)$ and for values of γ closer to zero there is a greater influence of the chaotic component and the encoded signal moves away from the message.

On the other hand, Figure 4 shows BER curves as a function of the channel SNR when using different values of γ and the quadratic map. For each value of SNR we simulated the transmission of 10^8 bits. To eliminate the transitory effect, the first 200 bits were discarded.

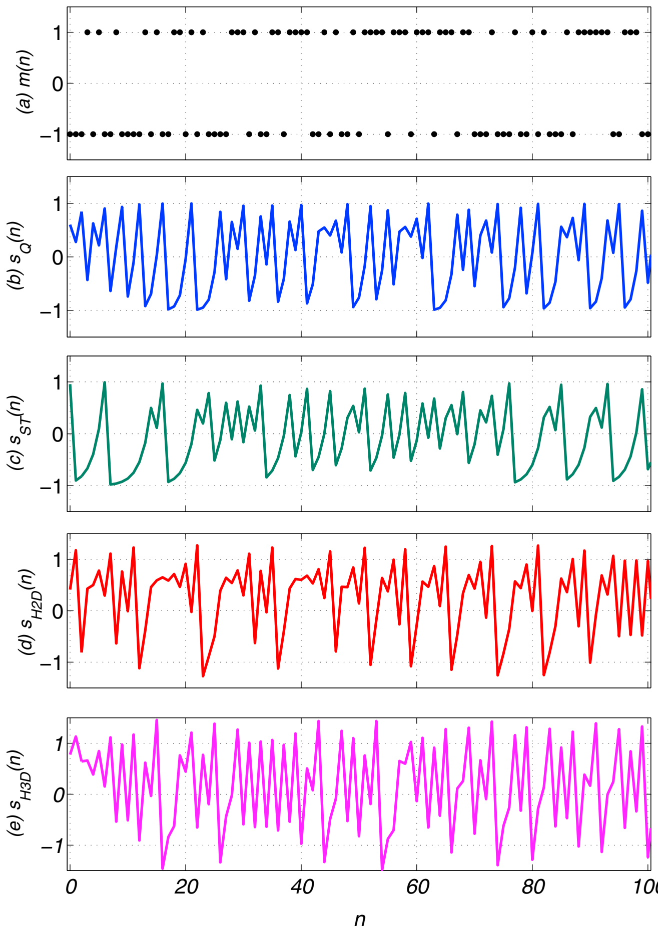

Fig. 2. Samples of transmitted signals in the system of Figure 1 using the encoding function (11) with $\gamma = 0.4$: (a) message $m(n)$ and $s(n)$ using (b) quadratic, (c) skew tent, (d) Hénon 2D and (e) Hénon 3D maps.

Analyzing this figure, we can notice that γ influences the results in terms of BER. When γ takes values close to zero, the BER only reach reasonable values in almost ideal channels. In contrast, for values of γ near the unity, we obtain the best results in terms of BER, next to the optimal case without chaos.

Thus, in Figures 3 and 4, it is observed that the value of γ represents a compromise between how much the message is hidden and the BER in AWGN. The optimal value of γ is the closest possible to unity, for lower BER, but as long as the message does not become apparent in the transmitted signal $s(n)$.

As an initial way to access how apparent is the message $m(n)$ in $s(n)$, we used as measure the BER that is obtained by applying a threshold decision *directly to the transmitted signal* $s(n)$, without decoding, in a noiseless channel. If $s(n) \approx m(n)$, a BER next to zero is expected and we conclude that the message is completely apparent in $s(n)$, i.e. there is no "security" whatsoever. If the message is hidden, a BER next to 0.5 is expected.

Figure 5 shows the BER values obtained in this way, as a function of γ for the different maps tested here. To carry out this simulation it was considered the transmission of 10^6 bits for each γ, random initial conditions and

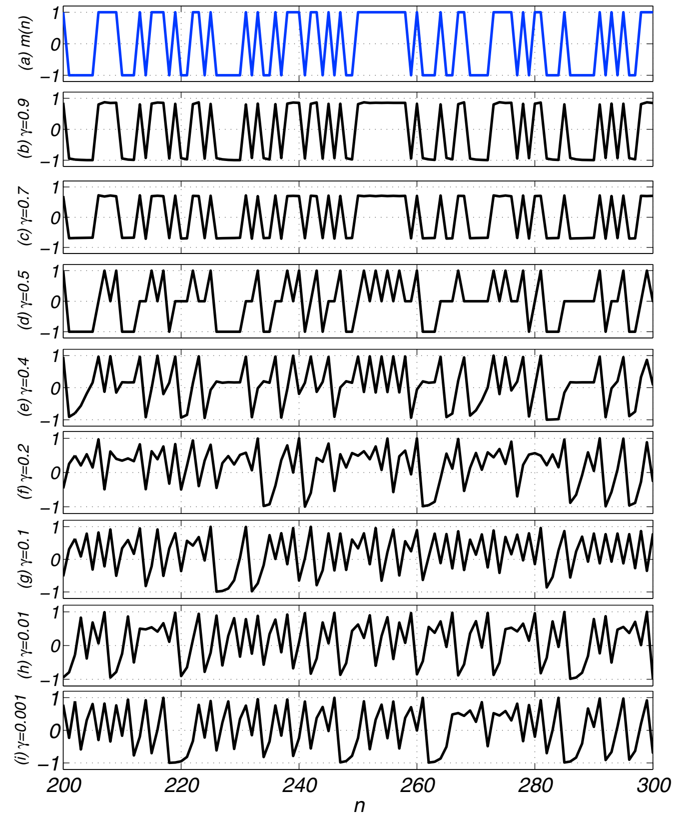

Fig. 3. Signal $s(n)$ generated from a message $m(n)$ using the quadratic map and encoding function (11) with different values of γ: (a) message $m(n)$ (samples were connected by straight line segments for clarity); transmitted signals $s(n)$ using (b) $\gamma = 0.9$, (c) $\gamma = 0.7$, (d) $\gamma = 0.5$, (e) $\gamma = 0.4$, (f) $\gamma = 0.2$, (g) $\gamma = 0.1$, (h) $\gamma = 0.01$ and (i) $\gamma = 0.001$.

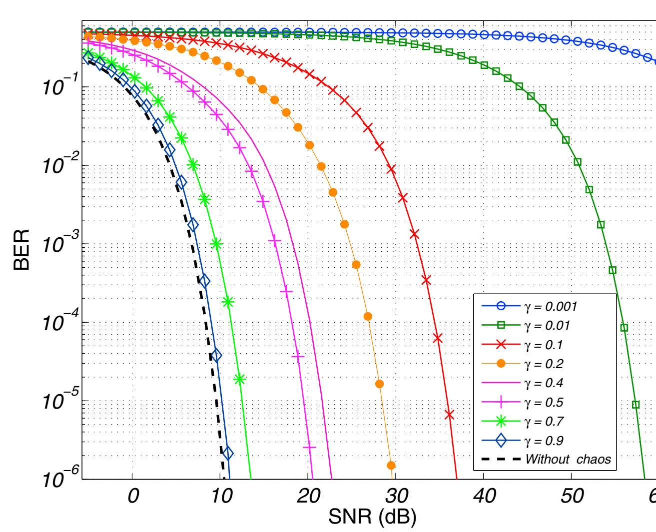

Fig. 4. BER as a function of SNR for the communication system studied using the quadratic map (14) and the values of γ from Fig. 3.

the first 200 bits were discarded. Notice that for the Hénon 3D map for $0 < \gamma \leq 0.01$ and $0.05 < \gamma < 0.35$, the signals generated diverge which prevents the choice of these intervals of γ for this particular map.

From this figure, $\gamma \approx 0.4$, is an interesting value to be considered as the BER obtained only with a threshold on the transmitted signal exceeding 30% for all maps used. Thus, $m(n)$ is sufficiently "hidden" and we still have a reasonable performance in AWGN channel, as shown in Figure 4. It is interesting to notice that previous works that consider similar chaos modulation schemes (see e.g. (Eisencraft et al., 2009; Cuomo and Oppenheim, 1993; Cuomo et al., 1993)) use to consider much lower values of γ. This is due to the fact that, in general, they concern only with the "security" of the system and do not take into account its BER performance in AWGN.

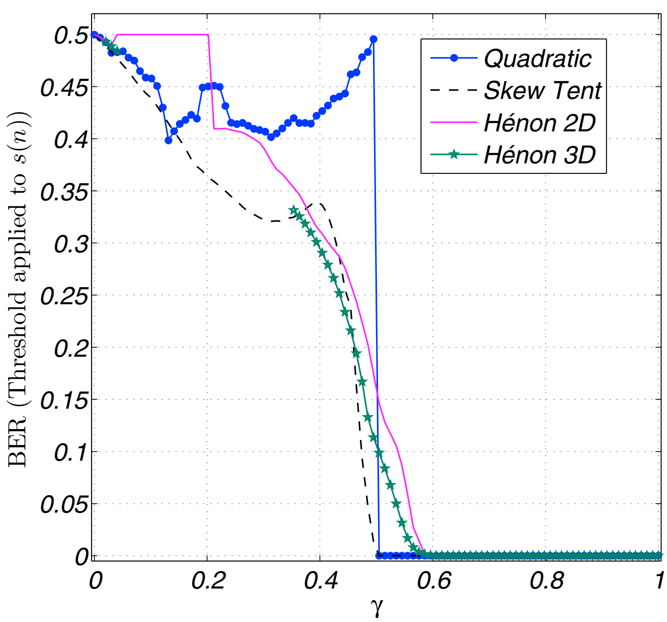

Fig. 5. BER obtained with threshold applied directly to $s(n)$ as function of γ. The signals generated by the Hénon 3D map diverge for some values of γ. At these points the curve is not shown.

Figure 6 shows BER curves for the employed maps with $\gamma = 0.4$. It was considered the transmission of 10^8 bits for each SNR, random initial conditions and the first 200 bits were discarded. We notice that, for $\gamma = 0.4$, the skew-tent map shows BER values below that of other maps for higher values of SNR. Using the encoding function with an appropriate value of γ, the curves are much closer to the optimal result *without chaos* than in others communication systems based on chaos synchronization previously described in the literature (Williams, 2001).

5. CONCLUSIONS

In this paper, we analyze the performance in terms of BER of a digital chaos-based communication system in AWGN channel. Four different maps and an innovative encoding function were tested. The proposed function has a parameter that allows to control the trade-off between how apparent is the message in the transmitted signal and the BER performance. It was numerically shown that it is possible to choose a parameter of the encoding function so that the message is not apparent and the BER values in AWGN channel are suitable for practical communications.

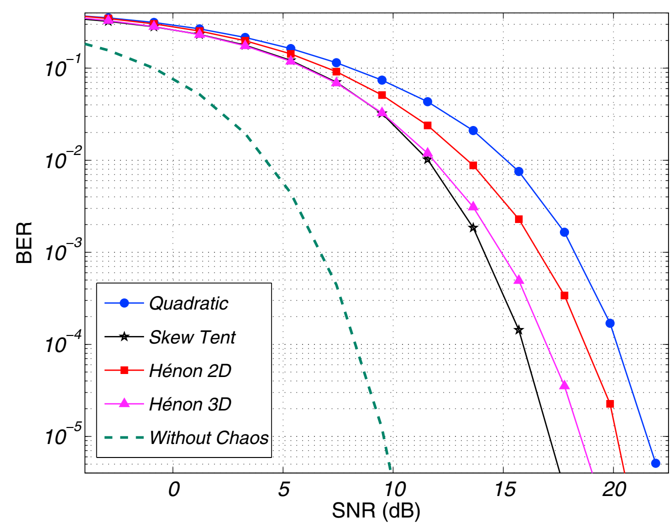

Fig. 6. BER as a function of SNR for $\gamma = 0.4$.

The results presented in this work are still below of what is obtained with conventional systems, at least in terms of BER in AWGN channel. As alternatives to improve this performance and as suggestion for future works it can be considered to explore concepts of bio-inspired algorithms (Soriano et al., 2012a), reservoir dynamics (Schrauwen et al., 2007) and networks of maps (Eisencraft and Batista, 2011) to improve the robustness to noise of chaotic synchronization. Another relevant topic as future work is to better define the concept of "hidden" messages, comparing the gains in terms of security in using a chaos-based technique with conventional cryptography and security at the physical layer.

REFERENCES

Agarwal, R.P. (1992). *Difference equations and inequalities*, volume 155 of *Monographs and Textbooks in Pure and Applied Mathematics*. Marcel Dekker Inc., New York. Theory, methods, and applications.

Alligood, K., Sauer, T., and Yorke, J. (1997). *Chaos: An Introduction to Dynamical Systems*. Textbooks in Mathematical Sciences. Springer.

Argyris, A., Syvridis, D., Larger, L., Annovazzi-Lodi, V., Colet, P., Fischer, I., Garcia-Ojalvo, J., Mirasso, C.R., Pesquera, L., and Shore, K.A. (2005). Chaos-based communications at high bit rates using commercial fibre-optic links. *Nature*, 438(7066), 343–346.

Boccaletti, S., Kurths, J., Osipov, G., Valladares, D., and Zhou, C. (2002). The synchronization of chaotic systems. *Physics Reports*, 366, 1 – 101.

Cuomo, K.M. and Oppenheim, A.V. (1993). Circuit implementation of synchronized chaos with applications to communications. *Phys. Rev. Lett.*, 71(1), 65–68. doi: 10.1103/PhysRevLett.71.65.

Cuomo, K., Oppenheim, A., and Strogatz, S.H. (1993). Synchronization of lorenz-based chaotic circuits with applications to communications. *Circuits and Systems II: Analog and Digital Signal Processing, IEEE Transactions on*, 40(10), 626–633. doi:10.1109/82.246163.

Dmitriev, A., Kletsov, A., Laktyushkin, A., Panas, A., and Starkov, S. (2006). Ultrawideband wireless communications based on dynamic chaos. *Journal of Communi-*

cations Technology and Electronics, 51(10), 1126–1140. doi:10.1134/S1064226906100020.

Eisencraft, M. and Batista, A.M. (2011). Discrete-time chaotic systems synchronization performance under additive noise. *Signal Processing*, 91(8), 2127 – 2131. doi: 10.1016/j.sigpro.2011.01.021.

Eisencraft, M., Fanganiello, R.D., Grzybowski, J.M.V., Soriano, D.C., Attux, R.F., Batista, A.M., Macau, E.E.N., Monteiro, L.H.A., Romano, J.M.T., Suyama, R., and Yoneyama, T. (2012). Chaos-based communication systems in non-ideal channels. *Communications in Nonlinear Science and Numerical Simulation*, 17(12), 4707 – 4718. doi:10.1016/j.cnsns.2011.05.030.

Eisencraft, M., Kato, D.M., and Monteiro, L.H.A. (2010). Fast communication: Spectral properties of chaotic signals generated by the skew tent map. *Signal Process.*, 90(1), 385–390. doi: http://dx.doi.org/10.1016/j.sigpro.2009.06.018.

Eisencraft, M., Attux, R.R.F., and Suyama, R. (eds.) (2013). *Chaotic Signals in Digital Communications*. CRC Press, Inc.

Eisencraft, M., Fanganiello, R.D., and Baccalá, L.A. (2009). Synchronization of Discrete-Time Chaotic Systems in Bandlimited Channels. *Mathematical Problems In Engineering*, 2009, 1–13. doi:10.1155/2009/207971.

Grzybowski, J.M.V., Rafikov, M., and Macau, E.E.N. (2010). Chaotic communication on a satellite formation flying–the synchronization issue in a scenario with transmission delays. *Acta Astronautica*, 66(7-8), 1160 – 1168. doi:10.1016/j.actaastro.2009.10.010.

Grzybowski, J.M.V., Eisencraft, M., and Macau, E.E.N. (2011). Chaos-based communication systems: Current trends and challenges. In S. Banerjee, M. Mitra, and L. Rondoni (eds.), *Applications of Chaos and Nonlinear Dynamics in Engineering - Vol. 1*, volume 71 of *Understanding Complex Systems*, 203–230. Springer Berlin / Heidelberg. 10.1007/978-3-642-21922-1_7.

Hénon, M. (1976). A two-dimensional mapping with a strange attractor. *Communications in Mathematical Physics*, 50, 69–77. 10.1007/BF01608556.

Kennedy, M.P., Setti, G., and Rovatti, R. (eds.) (2000). *Chaotic Electronics in Telecommunications*. CRC Press, Inc., Boca Raton, FL, USA.

Lathi, B. and Ding, Z. (2009). *Modern Digital and Analog Communication Systems*. The Oxford Series in Electrical and Computer Engineering. Oxford University Press, Incorporated.

Lau, F.C.M. and Tse, C.K. (2003). *Chaos-based digital communication systems*. Springer, Berlin.

Monteiro, L.H.A., Lisboa, A., and Eisencraft, M. (2009). Route to chaos in a third-order phase-locked loop network. *Signal Processing*, 89(8), 1678 – 1682. doi: 10.1016/j.sigpro.2009.03.006.

Oppenheim, A.V. and Schafer, R.W. (2009). *Discrete-Time Signal Processing*. Prentice Hall Press, Upper Saddle River, NJ, USA, 3rd edition.

Ren, H.P., Baptista, M.S., and Grebogi, C. (2013). Wireless communication with chaos. *Phys. Rev. Lett.*, 110, 184101. doi:10.1103/PhysRevLett.110.184101.

Rovatti, R., Mazzini, G., and Setti, G. (2004). On the ultimate limits of chaos-based asynchronous ds-cdma-i: basic definitions and results. *IEEE Trans. Circuits Syst. I*, 51(7), 1336–1347.

Schrauwen, B., Verstraeten, D., and Campenhout, J.M.V. (2007). An overview of reservoir computing: theory, applications and implementations. In *The European Symposium on Artificial Neural Networks*, 471–482.

Soriano, D.C., Abib, G.A., Eisencraft, M., Attux, R., and Suyama, R. (2012a). Using an evolutionary denoising approach to improve the robustness of chaotic synchronization. In *Proceedings of the third IFAC CHAOS Conference*, 128–132. International Federation of Automatic Control (IFAC), International Federation of Automatic Control (IFAC).

Soriano, D.C., Nadalin, E.Z., Suyama, R., Romano, J.M., and Attux, R. (2012b). Chaotic convergence of the decision-directed blind equalization algorithm. *Communications in Nonlinear Science and Numerical Simulation*, 17(12), 5097 – 5109. doi: http://dx.doi.org/10.1016/j.cnsns.2012.05.015.

Williams, C. (2001). Chaotic communications over radio channels. *Circuits and Systems I: Fundamental Theory and Applications, IEEE Transactions on*, 48(12), 1394 –1404. doi:10.1109/TCSI.2001.972846.

Wu, C.W. and Chua, L.O. (1993). A simple way to synchronize chaotic systems with applications to secure communication systems. *International Journal of Bifurcation and Chaos*, 3(6), 1619–1627. doi: 10.1142/S0218127493001288.